ACS Biomaterials SCIENCE & ENGINEERING

pubs.acs.org/journal/abseba

Article

Robust Antigen-Specific T Cell Activation within Injectable 3D Synthetic Nanovaccine Depots

Jorieke Weiden, Marjolein Schluck, Melina Ioannidis, Eric A. W. van Dinther, Mahboobeh Rezaeeyazdi, Fawad Omar, Juulke Steuten, Dion Voerman, Jurjen Tel, Mustafa Diken, Sidi A. Bencherif, Carl G. Figdor, and Martijn Verdoes*

Cite This: *ACS Biomater. Sci. Eng.* 2021, 7, 5622–5632

Read Online

ACCESS | Metrics & More | Article Recommendations | Supporting Information

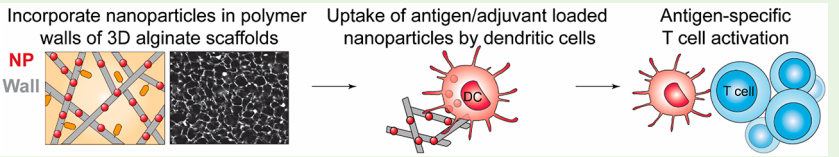

ABSTRACT: Synthetic cancer vaccines may boost anticancer immune responses by co-delivering tumor antigens and adjuvants to dendritic cells (DCs). The accessibility of cancer vaccines to DCs and thereby the delivery efficiency of antigenic material greatly depends on the vaccine platform that is used. Three-dimensional scaffolds have been developed to deliver antigens and adjuvants locally in an immunostimulatory environment to DCs to enable sustained availability. However, current systems have little control over the release profiles of the cargo that is incorporated and are often characterized by an initial high-burst release. Here, an alternative system is designed that co-delivers antigens and adjuvants to DCs through cargo-loaded nanoparticles (NPs) incorporated within biomaterial-based scaffolds. This creates a programmable system with the potential for controlled delivery of their cargo to DCs. Cargo-loaded poly(D,L-lactic-*co*-glycolic acid) NPs are entrapped within the polymer walls of alginate cryogels with high efficiency while retaining the favorable physical properties of cryogels, including syringe injection. DCs cultured within these NP-loaded scaffolds acquire strong antigen-specific T cell-activating capabilities. These findings demonstrate that introduction of NPs into the walls of macroporous alginate cryogels creates a fully synthetic immunostimulatory niche that stimulates DCs and evokes strong antigen-specific T cell responses.

KEYWORDS: *biomaterial-based scaffolds, nanoparticles, cancer vaccination, dendritic cells, antigen-specific T cells*

INTRODUCTION

Cancer vaccination aims to enhance the magnitude and broaden the scope of the anticancer T cell repertoire by exploiting dendritic cells (DCs) as orchestrators of adaptive immune responses. By supplying DCs with a source of tumor-associated antigens and DC-activating adjuvants, such as toll-like receptor (TLR) ligands, DCs are equipped to (cross-)present antigens together with co-stimulatory cues to tumor-specific T cells. The vaccine formulation and the vaccine platform that is applied dictate the ability of their cargo (*i.e.*, immunostimulatory factors) to reach DCs *in vivo*. Moreover, the immunological context plays an important role as immunosuppressive environments will negatively impact DC maturation and T cell priming.[1]

Over the last years, biomaterial-based three-dimensional (3D) scaffolds have been applied for local immunotherapy to create permissive environments that exert spatiotemporal control over immunomodulatory cues and immune cells while minimizing off-target exposure to immune-activating agents.[2] Biomaterial-based scaffolds can be applied as cancer vaccines by locally implanting or injecting a physical 3D structure underneath the skin that recruits DCs through release of chemotactic factors such as granulocyte-macrophage colony-stimulating factor (GM-CSF).[3−9] The matrix provides incoming DCs with a depot of tumor-associated antigens (in the form of tumor lysates,[3] irradiated tumor cells,[4] or full protein either in soluble form adsorbed onto the scaffold[5,6,8] or covalently immobilized on the scaffold[7]) together with immune-stimulating adjuvants such as TLR 9 agonist CpG oligodeoxynucleotides. These scaffold-based approaches evoke potent and durable anti-cancer immunity in prophylactic and therapeutic preclinical models.[3−8] Immune responses were superior to subcutaneous administration of soluble antigens and adjuvants without scaffolds, suggesting that sustained availability, co-presentation of antigens/adjuvants, and the supportive environment provided by the matrix contribute to the induction of anti-cancer immune responses. However, the

Received: November 24, 2020
Accepted: October 21, 2021
Published: November 4, 2021

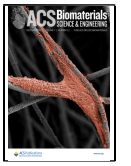

https://doi.org/10.1021/acsbiomaterials.0c01648
ACS Biomater. Sci. Eng. 2021, 7, 5622−5632

current systems have limited control over the release profiles of antigens and/or adjuvants that are incorporated and are often associated with an initial high burst release. Hence, there is a need to develop novel strategies to deliver cargo in a more controlled fashion to DCs within such scaffolds.

Incorporating antigens and adjuvants into nanoparticles (NPs) that are loaded into the scaffold walls provides a means to fine-tune their release profiles and degradation behavior, thereby providing an opportunity for another level of spatiotemporal control over the presentation of activating cues to DCs.[10] A particle-based approach furthermore benefits from the inherent uptake of particulate matter by DCs, thereby potentially improving uptake of the cargo,[11,12] favoring co-delivery of components for strong DC activation,[13−17] and enhancing cross-presentation[12,18−20] of antigens and adjuvants presented within biomaterial-based scaffolds. Thus, NPs may be exploited to trigger cancer-specific immune responses of enhanced magnitude and potency compared to delivery of soluble antigens and adjuvants.[10,19,21,22]

Here, we introduce an alternative strategy to co-deliver tumor-associated antigens and adjuvants to DCs. We expand on previous approaches by incorporating poly(D,L-lactic-*co*-glycolic acid) (PLGA) NPs carrying model tumor-associated antigens and two synthetic TLR ligands into the polymer walls of a scaffold-based delivery system. We make use of injectable macroporous cryogels based on alginate, a biocompatible and natural polysaccharide derived from algae, which have been reported to support immune cell infiltration and can be delivered in a minimally invasive manner through syringe injection.[4,23−25] Our findings demonstrate that PLGA NPs can be easily incorporated into macroporous alginate cryogels to create a fully synthetic immune niche that can stimulate DCs and evoke strong antigen-specific immune responses *in vitro*. This straightforward approach provides an important expansion of the scaffold-based vaccine platform which supports sustained presentation of antigens and adjuvants within a supportive environment and at the same time enables enhanced control over the uptake and release kinetics of antigens and adjuvants toward DCs.

EXPERIMENTAL SECTION

Methacrylation of Alginate. Methacrylated alginate (MA-alginate) was prepared, as described previously[4,23] with minor modifications. In brief, sodium alginate (Pronova UP LVG, NovaMatrix) was dissolved in a 100 mM 2-(*N*-morpholino)-ethanesulfonic acid (MES) buffer solution (pH 6.5). *N*-Hydroxysuccinimide (NHS, Sigma-Aldrich) (1.3 g) and *N*-(3-dimethylaminopropyl)-*N*′-ethylcarbodiimide hydrochloride (EDC, Sigma-Aldrich) (2.8 g) were added to activate the carboxylic acid groups of alginate. After 5 min, *N*-(3-aminopropyl)methacrylamide hydrochloride (APMA, Polysciences) (2.07 g; molar ratio of NHS/EDC/APMA is 1:1.3:1.1) was added to the solution. After 24 h stirring at room temperature (RT), the solution was precipitated in acetone, filtered, and dried on an oil pump. The degree of methacrylation of alginate was determined using ^{1}H NMR (Bruker Avance III 400 MHz, Figure S1A). The efficiency of methacrylation was determined based on the ratio of the integrals for alginate protons to the methylene protons.

Production of PLGA NPs. PLGA NPs were produced, as described previously using an o/w emulsion and solvent evaporation−extraction method.[13] PLGA NPs were prepared encapsulating endograde ovalbumin (OVA) protein (Hyglos) or NY-ESO-1 long peptide (long peptide covering the NY-ESO-1 HLA-A2.1 epitope SLLWITQC, GenScript) together with TLR ligands, polyinosinic/polycytidylic acid (polyI/C, Sigma-Aldrich), R848 (Enzo Life Sciences), and ATTO647N dye (A647, ATTO-TEC). The encapsulation efficiency of R848, NY-ESO-1 peptide, and A647 was determined by reverse-phase HPLC, as described previously.[13] R848, NY-ESO-1 peptide, or ATTO647N dye were extracted from NPs by dissolving 1 mg of NPs in 100 mL of dimethyl sulfoxide (DMSO) followed by centrifugation at 14,000 rpm for 10 min. A total of 25 μL of supernatant or standard was assayed by HPLC. The quantity of R848, NY-ESO-1 peptide, or ATTO647N dye was calculated by interpolation from the standard curves. The encapsulation efficiency of polyI/C was determined by absorption of digested particles or standard on a NanoDrop 2000 (Thermo Fischer Scientific), as described previously.[13] OVA amounts were quantified by measuring the protein content of digested particles using the Coomassie Plus Protein Assay Reagent (Pierce), according to the manufacturer's protocol. NP size and polydispersity were determined using dynamic light scattering (NANO-flex, Particle Metrix).

Fabrication and Characterization of Alginate Cryogels. Macroporous cryogels were produced by redox-induced free-radical polymerization for 17 h at −20 °C of MA-alginate in Milli-Q water, as described previously[4,23] at [2.3% (wt/vol)] alginate in a Teflon-mold with 4 × 4 × 1 mm dimension pre-cooled at −20 or 4 °C. PLGA NPs (sonicated 3 × 30 s with Bioruptor, Diagenode) or endograde OVA protein with TLR ligands polyI/C (Sigma-Aldrich) and R848 (Enzo Life Sciences)] were added to the polymer solution before cryogelation. The amount of tetramethylethylenediamine (TEMED) {[0.04% (wt/vol)−0.5% (wt/vol)]} and ammonium persulfate (APS) {[0.18% (wt/vol)−0.28% (wt/vol)]} varied to enable freezing of the solution before polymerization took place. ACRL-PEG-G4RGDAS-SKY was synthesized, as described,[4] which was used as a comonomer [0.8% (wt/vol)] during polymerization to create cell-adhesive cryogels. After thawing, cryogels were washed in MQ (1×) and sterile PBS (100 μL, 5×) before performing cell experiments.

Macroscopic characterization of the gels was performed by fluorescence microscopy (Olympus FV1000 confocal laser scanning microscope or Leica DMI600B). Cells were stained with Hoechst 33342 (1:2000, Thermo Fischer Scientific). Injectability of 4 × 4 × 1 mm cryogels was assessed via an injection through hypodermic 16G needles together with 200 μL of PBS. Structural analysis of 4 × 4 × 1 mm alginate cryogels was performed using scanning electron microscopy on lyophilized cryogels that were coated with 5 nm platinum. The swelling ratio was determined on 8 × 5 mm cylindrical alginate cryogels, as previously reported.[23]

R848 Release from OVA/TLR NP and Alginate Cryogels. Alginate cryogels were produced in 100 μL volumes containing 312.5 μg of soluble OVA/TLR NPs (50 μg of OVA/TLR NPs per 16 μL) or OVA protein with TLR ligands (polyI/C and R848) added prior to cryogelation in levels comparable to the OVA/TLR NPs. Two alginate cryogels or soluble OVA/TLR NPs (625 μg) were incubated in 1 mL of MQ at 37 °C on a shaker for up to 7 days. Supernatant was taken at different timepoints, lyophilized, dissolved in 40 μL MQ, and analyzed using HPLC (Waters XSelect Peptide CSH C18 column) for R848 release.

Mice. Mice were housed at the Central Animal Laboratory (Nijmegen, the Netherlands) where food and water were provided ad libitum. This study was carried out in accordance with European legislation. Protocols were approved by the local authorities (CCD, The Hague, the Netherlands, approval number 10300) for the care and use of animals with related codes of practice.

Generation of Mouse Bone-Marrow-Derived DCs and *In Vitro* DC Activation. Bone-marrow-derived DCs (BMDCs) were generated from female and male 5−12-week-old C57BL/6J mice (Charles River) using either GM-CSF or FLT3 ligand. The femurs and tibia were flushed with BMDC medium [RPMI 1640 medium supplemented with 10% heat-inactivated fetal calf serum (FCS), 0.5% antibiotic−antimycotic, 2 mM L-glutamine, and 55 μM beta-mercaptoethanol (all Gibco)] to extract bone marrow. For the GM-CSF DCs, bone marrow cells (2 to 4 × 10^6 per Petridish) were cultured in 13 mL of BMDC medium containing 20 ng/mL GM-CSF. On day 3, 4 mL of additional BMDC medium with 37.2 ng/mL GM-CSF was added to the cells. On day 6, GM-CSF BMDCs were

https://doi.org/10.1021/acsbiomaterials.0c01648
ACS Biomater. Sci. Eng. 2021, 7, 5622−5632

harvested through gentle aspiration and counted. GM-CSF BDMCs were dissolved at 10×10^6/mL in BMDC medium. For the FLT3 ligand, DC bone marrow cells (15×10^6 per Petridish) were cultured in 10 mL of BMDC-FLT3L medium (BMDC medium containing 200 ng/mL FLT3 ligand and 5 ng/mL GM-CSF). On day 5, 5 mL of additional BMDC-FLT3L medium was added to the cells. On day 9, nonadherent cells were harvested and replated (3×10^6 cells per Petridish) in 10 mL of BMDC-FLT3L medium. On day 13, FLT3L BMDCs were harvested through gentle aspiration and counted. FLT3L BDMCs were dissolved at 10×10^6/mL in BMDC medium.

Alginate cryogels were placed in a sterile flat bottom 96 well plate (Corning), and when indicated, gels were incubated for 1 or 2 days in 200 μL BMDC medium at 37 °C prior to cell experiments. Following the incubation, gels were either dried with a sterile 5 × 5 Surgical Care HG Compress (Killion) and placed in a sterile flat bottom 96-well plate or directly placed in a sterile flat bottom 96-well plate. Subsequently, 1×10^5 day 6 GM-CSF BMDCs in 10 μL or 1×10^5 day 13 FLT3L BMDCs in 10 μL were added on top of the gels. After 1−2 h incubation, another 190 μL of medium was added to the wells. TLR ligands [soluble polyI/C (20 μg/mL) and R848 (4 μg/mL)] or sonicated PLGA NPs without scaffold were used as positive controls. Where indicated, TLR ligands and OVA proteins were added in amount similar to that present in PLGA NPs. Cells were incubated at 37 °C for 24 or 48 h, as indicated. The supernatant was collected for analysis of cytokine production by DCs. Both types of BMDCs were harvested by incubating them for 15 min at RT with 50−100 μL Accutase (Thermo Fisher Scientific). Thereafter, 100 μL of BMDC medium was added, and the gels were centrifuged at 200 rcf for 10 min and at 450 rcf for 2 min. Cryogels were carefully taken out, and cells were transferred to a V-bottom plate for antibody staining. Cells were stained with Zombie Violet Fixable viability dye (eBioscience) for 30 min at 4 °C, followed by cell-surface staining with the following antibodies for 30 min at 4 °C: CD11c-PE Cy7 (BD PharMingen) (purity typically >90%), CD80-FITC (BioLegend), CD40-PE (BD PharMingen), CD86-biotin (BD PharMingen), and BV510-conjugated streptavidin. Cell viability was assessed using Annexin V (BD PharMingen) and 7AAD staining (eBioscience) and compared to medium and collagen hydrogels generated, as described.[26] In all experiments, cells were analyzed using a BD FACSVerse flow cytometer, and data were analyzed using FlowJo software version 10.0.7.

Isolation of OT-I T Cells and Antigen-Specific Activation of OT-I T Cells by BMDCs. OT-I CD8α^+ T cells were isolated from 5−16 week old female and male OT-I mice [C57BL/6-Tg(TcraTcrb)-1100Mjb/Crl, Charles River]. Spleen, inguinal, and axillary lymph nodes were digested for 30 min at 37 °C with DNase I (20 μg/mL, Roche) and Collagenase III (1 mg/mL, Worthington) and subsequently meshed over a 100 μm cell strainer. Splenocytes were treated with ammonium−chloride−potassium lysis buffer for 3−5 min at RT to lyse blood cells. CD8α^+ T cells were isolated using the mouse CD8α^+ T cell isolation kit (Miltenyi Biotec), according to the protocol. Purity was typically >95%, as determined by flow cytometry staining with APC-conjugated CD8α (BioLegend). Next, OT-I cells were stained with CellTrace Violet (2, 5 μM; Invitrogen) for 10 min at 37 °C, according to the protocol.

To study antigen-specific OT-I T cell activation, 20,000 GM-CSF or FLT3L BMDCs were activated for 24 h in alginate cryogels or using positive controls. Next, 50,000 CellTrace Violet-labelled OT-I T cells were added. The supernatant was taken after 24 h of OT-I activation to determine IFNγ production, and after 72 h, cells were collected through incubation with 150 μL of cold PBS + 2 mM ethylenediaminetetraacetic acid for 10 min at 4 °C. Retrieved cells were stained with Fixable Viability Dye eFluor 780 (eBioscience) and CD8α-PE (BD PharMingen). The mean cell cycle of all T cells was determined as a measure for the average number of cell proliferation cycles. The mean cycle was calculated with the formula Log2(f), where f is the Cell Trace Violet geometric mean fluorescence intensity (MFI) of all non-proliferated T cells divided by the Cell Trace Violet MFI of all T cells. The division index was calculated using FlowJo software.

Generation of Human Monocyte-Derived DCs and *In Vitro* DC Activation. Peripheral blood mononuclear cells were isolated from buffy coats obtained from HLA-A2.1$^+$ healthy volunteers after written informed consent and in agreement with institutional guidelines using Ficoll density gradient centrifugation (Lymphoprep, ELITechGroup). CD14$^+$ monocytes and naïve CD8$^+$ T cells were isolated using CD14 microbeads and the human Naive CD8$^+$ T cell isolation kit (both Miltenyi Biotec), respectively. Monocytes were differentiated into immature monocyte-derived DCs (moDCs) in 6 days using RPMI 1640 containing 10% FCS, 2 mM L-glutamine, 0.5% antibiotic−antimycotic enriched with interleukin-4 (IL-4, 300 U/mL), and GM-CSF (450 U/mL) (both Miltenyi Biotec). Isolated cells were stored in liquid nitrogen in 10% DMSO (CryoSure) and 90% FBS.

Human moDCs were thawed from liquid nitrogen. *In vitro* DC activation (24 and 48 h) in alginate cryogels containing NY-ESO-1 PLGA NPs was studied, as described for BMDCs. Soluble NY-ESO-1 peptide and TLR ligands were added to the controls in the same amounts as is present in NPs. Flow cytometric staining was performed using Zombie Violet Fixable viability dye for 30 min at 4 °C, followed by cell-surface staining with the following antibodies for 30 min at 4 °C: CD14-FITC (Miltenyi Biotec), CD80-PerCP-eFluor710 (PharMingen), CD86-PeCy7 (PharMingen), and CD40-PE (Beckman).

CD8$^+$ T Cell Transfection and NY-ESO-1 Specific T Cell Activation by moDCs. CD8$^+$ T cells from the same HLA-A2.1$^+$ donor as the moDCs were transfected, as previously described[27] with mRNA (5 mg/mL, BioNTech RNA Pharmaceuticals) encoding for a mouse T cell receptor (specific for the HLA-A2.1-specific NY-ESO-1 epitope SLLWITQC). Transfection efficiency was determined 1 day after transfection using anti-mouse TCR-β-FITC (BioLegend) and was typically between 80 and 90% (Figure S9A). These NY-ESO-1 specific T cells were stained with CellTrace Violet and were added to activated moDCs (ratio DCs/T cells as 1:2.5) in alginate cryogels. The supernatant was taken after 24 h of T cell activation to determine IFNγ production. After 72 h of activation, cells were collected and stained with Fixable Viability Dye eFluor 780, CD8-FITC (BD BioScience), and CD25-PE (BD BioScience).

Migration of DCs through Alginate Cryogels. Immature moDCs were activated for 48 h with a mixture of IL-4 (300 U/mL), GM-CSF (450 U/mL), tumor necrosis factor α (TNFα, 10 ng/mL) (CellGenix), prostaglandin E2 (10 μg/mL) (Pfizer), IL-1β (5 ng/mL) (CellGenix), and IL-6 (15 ng/mL) (CellGenix). Approximately 1×10^5 day 8 mature moDCs were added on top of 75 μL collagen hydrogels generated, as described[26] or on top of 75 μL alginate cryogels alone or topped with 25 μL collagen in a transwell insert containing 5 μm pores (Corning). The lower chamber of the transwell system was supplemented with 1 μg/mL CCL21 (BioLegend), which was refreshed after 24 h. The number of migrated moDCs were quantified after 48 h using the MACS Quant analyzer (Miltenyi Biotec).

Production of Cytokines. Cytokine production by mouse and human DCs and T cells was quantified using standard sandwich ELISA kits, according to the manufacturer's protocol. Mouse IL-6 (BioLegend), TNFα (eBioscience), IFNγ (Invitrogen), IL-12 (Invitrogen), and human IFNγ (Invitrogen) were determined.

Statistical Analysis. Data are expressed as mean ± standard error of the mean. Statistical analyses were performed in GraphPad Prism 6 software using the appropriate testing methods, as indicated in the figure legends. Statistical significance was defined as a two-sided significance level of <0.05. ns = not significant, $*p \leq 0.05$, $**p \leq 0.01$, and $***p \leq 0.001$.

RESULTS

Production of PLGA NP-Loaded Alginate Cryogels. We probed the potential of alginate cryogels to serve as a scaffold-based depot of tumor antigens and adjuvant-loaded PLGA NPs. Alginate is an attractive basis for biomaterial-based scaffolds as alginate polysaccharides are non-immunogenic, non-toxic, and biocompatible.[28] Macroporous 3D scaffolds

https://doi.org/10.1021/acsbiomaterials.0c01648
ACS Biomater. Sci. Eng. 2021, 7, 5622−5632

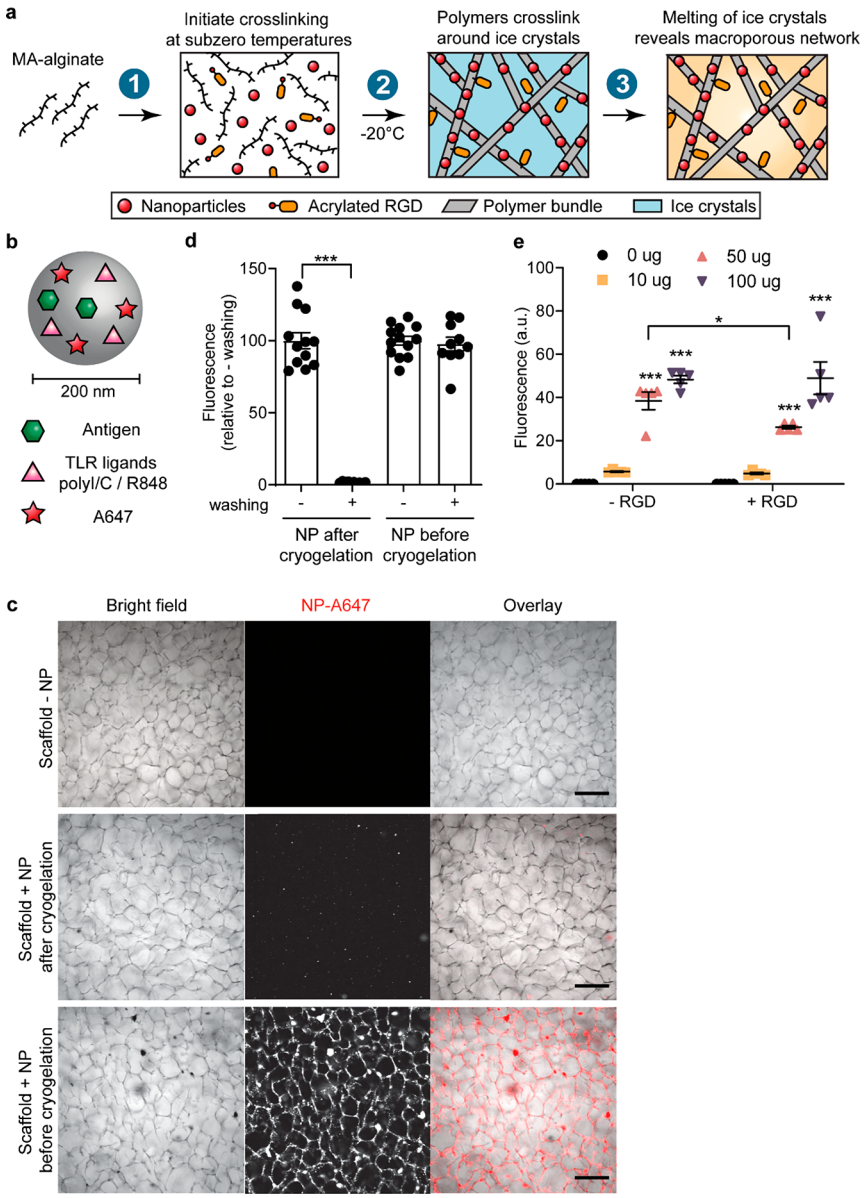

Figure 1. Production of PLGA NP-loaded alginate cryogels. (A) Schematic overview of the cryogelation process. (B) Schematic overview of antigen and adjuvant-loaded PLGA NPs. (C) Representative confocal images of alginate cryogels prepared in polystyrene molds without OVA/TLR NP PLGA NPs (upper panels), PLGA NPs added after (middle panels), or before (bottom panels) cryogelation. Scale bar equals 100 μm. (D) Quantification of A647 fluorescence of 4 × 4 × 1 mm cryogels where 50 μg of OVA/TLR NPs was added (cryogels before washing set to 100%). Data were analyzed with an unpaired *t*-test to compare with and without washing. (E) Fluorescence of OVA/TLR A647-NPs incorporated into alginate cryogels with or without [0.8% (wt/vol)] RGD. A two-way ANOVA with Dunnett's multiple comparison test (comparing NP concentration) or Sidak's multiple comparisons test (comparing −RGD and +RGD) was performed to test statistical significance. (D,E) Stars indicate significance compared to 0 μg, unless indicated otherwise.

were prepared through free-radical cross-linking of methacrylated alginate polymers (MA-alginate, Figure S1A) at −20 °C to create a large and interconnected porous structure that facilitates influx of cells. During the cryopolymerization process, MA-alginate polymers and PLGA NPs are concentrated in semi-frozen regions around the ice crystals (Figure 1A). Cross-linking of MA-alginate proceeds within these semi-frozen regions, resulting in the physical entrapment of PLGA NPs within the tightly cross-linked polymer walls of the alginate scaffold. Ice crystals act as porogens and their size and structure dictate the nature of the macroporous network of the resulting 3D cryogels.[23]

The PLGA NPs that were incorporated into the polymer walls of alginate cryogels have been frequently used for DC activation.[10,13] These particles are negatively charged and are approximately 200 nm in size and contain TLR3 ligand polyI/C, TLR7/8 ligand R848, and an A647 fluorescent dye. In addition, as antigens we added either OVA protein (OVA/TLR NPs), which can be used in preclinical tumor mouse models, or a clinically relevant human NY-ESO-1 long peptide (NY-ESO-1/TLR NPs) (Figures 1B and S1B,C).

To construct cell-adhesive scaffolds that facilitate the interaction with cellular integrin receptors, acrylated RGD peptide ligands were co-polymerized during the cryogelation process.[29]

https://doi.org/10.1021/acsbiomaterials.0c01648
ACS Biomater. Sci. Eng. 2021, 7, 5622−5632

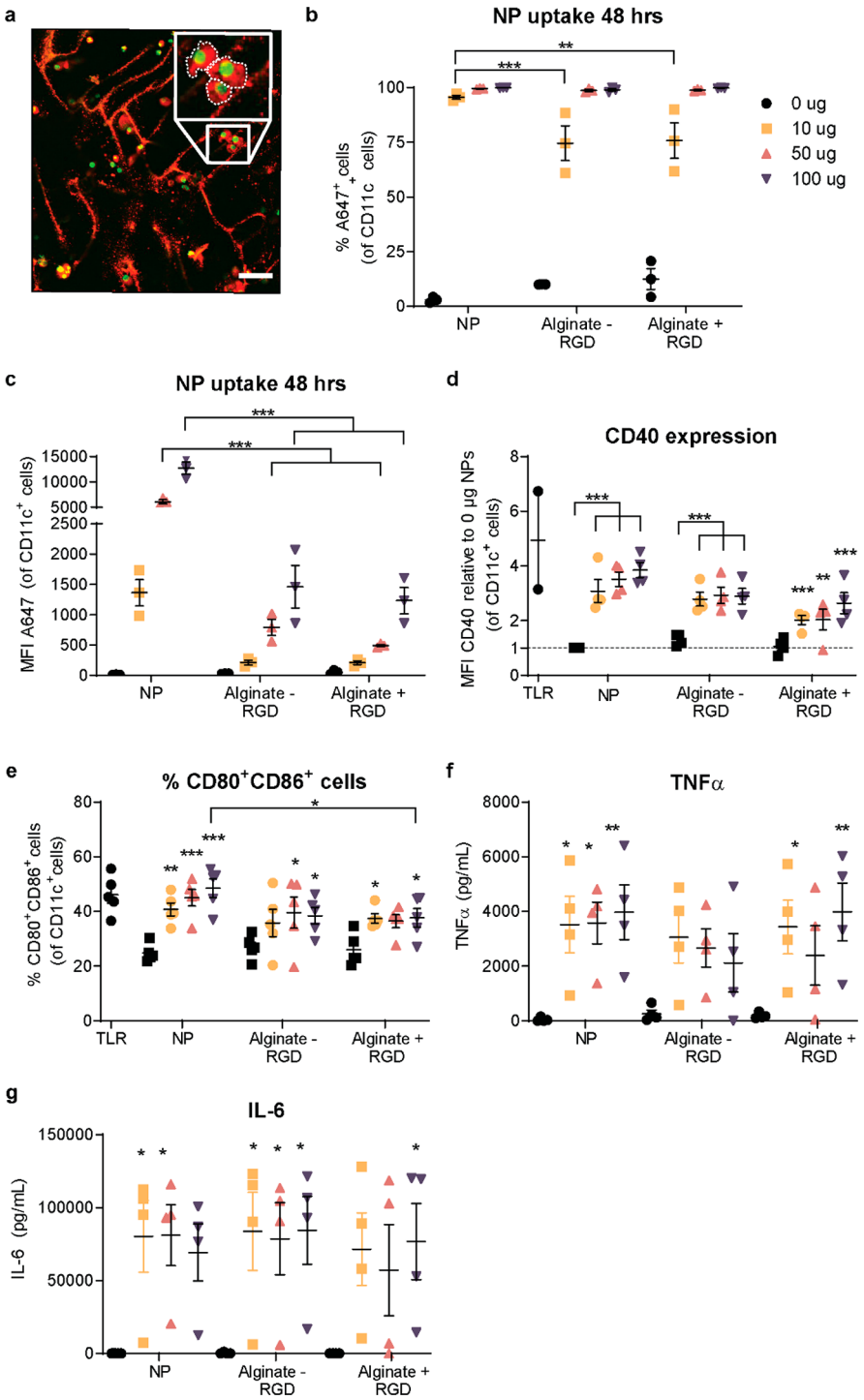

Figure 2. Mouse BMDCs take up PLGA NPs from alginate cryogels which induces DC maturation. (A) Representative confocal image of BMDCs in OVA/TLR A647-NP-loaded alginate cryogel [green = nuclei (Hoechst), red = A647 dye from NPs] after 24 h. Scale bar equals 50 μm. Inset: Dotted line represents outline of cell. (B−G) BMDCs were cultured 48 h with OVA/TLR A647-NPs or NPs encapsulated in alginate cryogel polymer walls with or without [0.8% (wt/vol)] RGD, after which the % of A647$^+$ cells (B), A647 geometric MFI (C), CD40 MFI (D), and the % CD80$^+$CD86$^+$ cells (E) of CD11c$^+$ cells were determined. The amount of TNFα (F) and IL-6 (G) in the supernatant after 24 h was quantified. (B,C) n = 3 in three independent experiments. (D,F,G) n = 4 in four independent experiments. (B−G) Data were analyzed using a two-way ANOVA and Dunnett's multiple comparison test. Stars indicate significance compared to 0 μg, unless indicated otherwise.

We added OVA/TLR NPs to the MA-alginate solution before induction of free-radical polymerization and investigated NP localization in the alginate network using confocal microscopy after washing of the scaffolds. The retention of NPs was observed, and they exclusively localized in association with the walls of the scaffold. In contrast, addition of NPs after the cryogelation process to pre-formed cryogels did not result in particle retention after washing (Figure 1C). To quantitatively corroborate this observation, the A647 fluorescence signal before and after washing of the respective alginate cryogels was measured. This analysis demonstrated that >97% of NPs are retained within the cryogels after

https://doi.org/10.1021/acsbiomaterials.0c01648
ACS Biomater. Sci. Eng. 2021, 7, 5622−5632

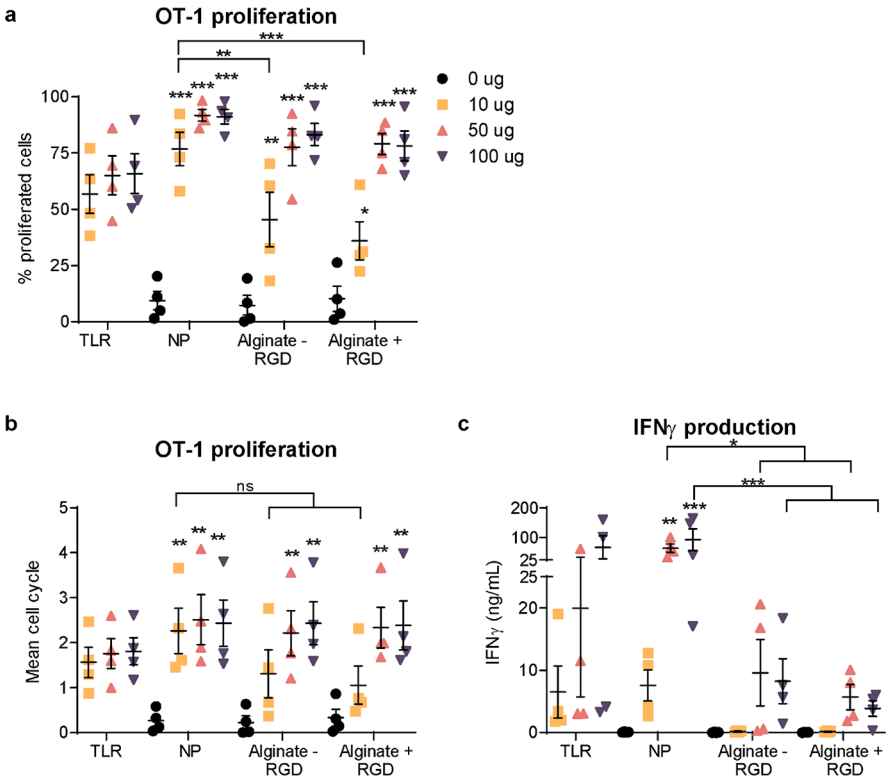

Figure 3. Mouse BMDCs acquire antigen-specific T cell-priming capabilities within NP-loaded scaffolds. (A–C) OT-I T cells were added to BMDCs cultured in alginate cryogels and the % of proliferated OT-I T cells (A) and their mean cell cycle (B) after 72 h was determined, together with their IFNγ production after 24 h (C). In the "TLR" conditions, equal amounts of soluble OVA were added as in 10, 50, or 100 μg NPs, together with R848/polyI/C (A–C) $n = 4$ in four independent experiments. Data were analyzed using a two-way ANOVA and Dunnett's multiple comparisons test. Stars indicate significance compared to 0 μg, unless indicated otherwise.

repeated washing when the NPs were added before cross-linking, whereas most of the fluorescence was washed away when the NPs were added to the preformed cryogels (Figure 1D). This indicates that NPs do not simply stick to the polymers as was pursued previously[30] but instead are entrapped within the dense scaffold walls when they are added prior to cryogelation. We next evaluated NP encapsulation at different doses into non-functionalized alginate cryogels and adhesive RGD-functionalized cryogels. A clear dose-dependent increase in fluorescence was observed with increasing amounts (0–100 μg) of OVA/TLR NPs. This observed increase in fluorescence was similar for cryogels with and without adhesion sites (Figure 1E). In conclusion, NPs were successfully encapsulated within the polymer walls of alginate cryogels with or without cell adhesion moieties by introducing them to the free polymer solution before cryogelation with a high encapsulation efficiency.

Mechanical Properties of NP-Loaded Cryogels. Alginate cryogels are highly elastic and display remarkable deformability. They shear-collapse when force is applied and re-gain their shape when the stress is relieved.[23] The cryogelation process determines the mechanical properties of the scaffold. In particular, balancing ice nucleation and freezing rate *versus* the rate of free-radical polymerization is pivotal.

We hypothesized that addition of NPs to the polymer solution may affect the cryogelation process and could thus impact the injectability of the cryogels as a whole. Therefore, we investigated whether introducing NPs into the polymer network would affect cryogel integrity and mechanical properties when using the cryo-polymerization conditions described above. Although the PLGA NPs are small enough to fit within the porous walls of the scaffolds, addition of 50 or 100 μg of PLGA NPs altered the cryogel structure on a macroscopic level and affected mechanical robustness, resulting in breaking during injection (Figure S2A,B). Most likely the presence of NPs in the polymer solution affects the rate of ice nucleation and thereby alters the scaffold network structure. Decreasing the amount of the polymerization initiator system (APS and TEMED) and thereby slowing down the gelation process and effectively providing more time for nucleation and growth of ice crystals indeed restored scaffold integrity and rescued scaffold injectability through a 16G needle (Figure S2C). The presence of NPs did not significantly impact the swelling ratio of alginate cryogels (Figure S2D). These results suggest that by careful tuning of the polymerization initiator system, mechanically robust alginate cryogels with high amounts of NPs can be produced.

Murine DC and T Cell Activation in OVA/TLR NP-Loaded Alginate Cryogels. To establish whether PLGA NPs entrapped within tightly cross-linked alginate cryogel polymer walls are available for DCs, we cultured mouse BMDCs in OVA/TLR NP-loaded alginate cryogels and studied their ability to take up NP-encapsulated cargo. BMDCs remained viable within the scaffolds (Figure S3A), and cryogel porosity permitted DC infiltration and migration throughout the construct (Figure S3B). These observations together with the similar porosity, similar matrix interconnectivity, and similar injectability (Figure S2) that we observed for the NP-loaded cryogels compared to non-NP-loaded cryogels suggest that the NP-loaded will effectively allow for the influx

https://doi.org/10.1021/acsbiomaterials.0c01648
ACS Biomater. Sci. Eng. 2021, 7, 5622–5632

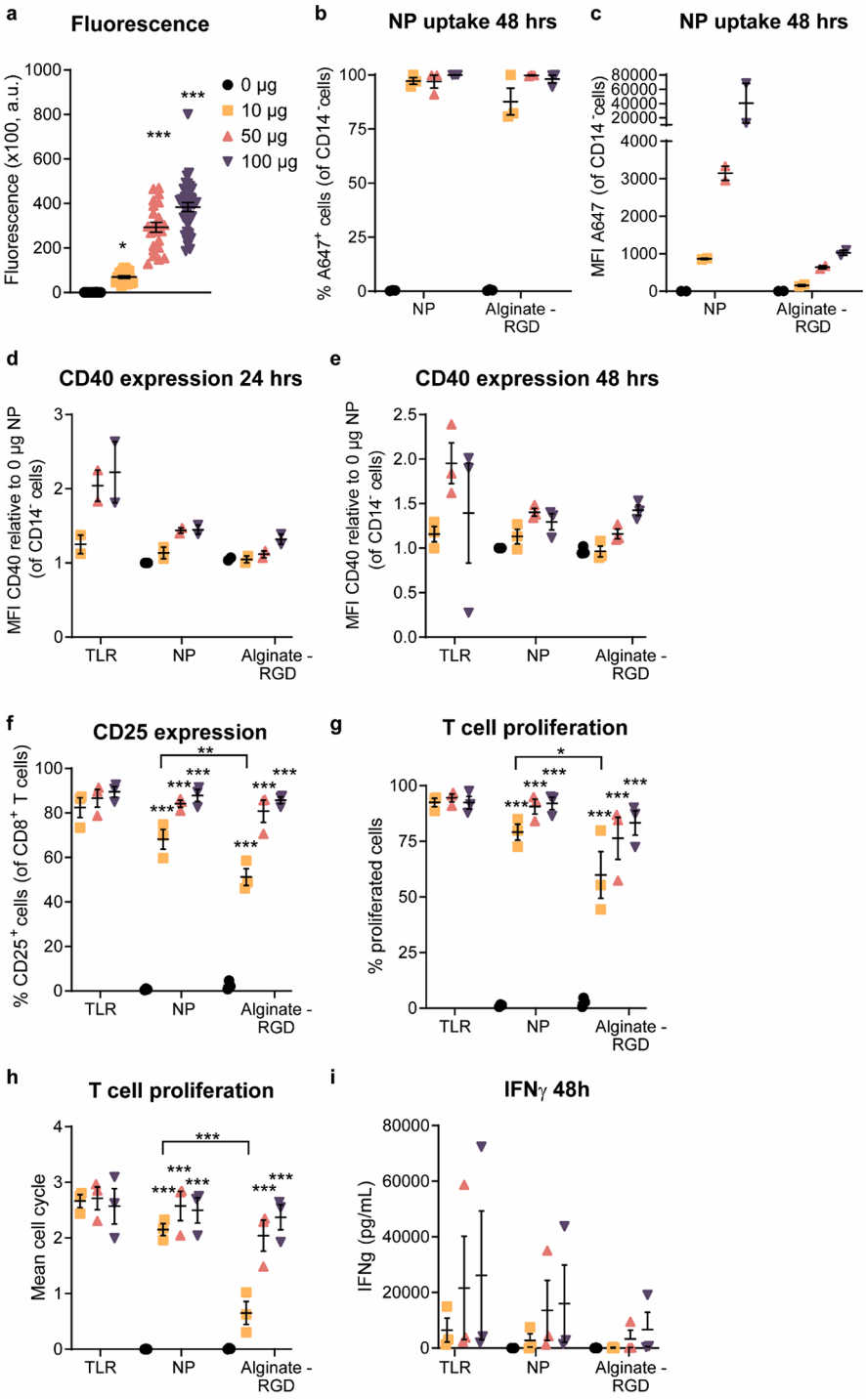

Figure 4. Human moDCs activated by PLGA NP-loaded alginate cryogels prime NY-ESO-1-specific T cells. (A) Fluorescence of NY-ESO-1/TLR A647-NPs incorporated into alginate cryogels. A Kruskal−Wallis test and Dunn's multiple comparison test were performed to test statistical significance. $n \geq 23$ in three independent experiments. (B−E) Human moDCs were cultured for 24 or 48 h with NY-ESO-1/TLR A647-NPs or NPs incorporated into alginate cryogels, after which the percentage of A647$^+$ cells (B), A647 MFI (C), and relative CD40 MFI (D,E) in CD14$^-$ viable cells was determined. The same amount of soluble NY-ESO-1 and soluble TLR ligands was used in "TLR" conditions as in 10, 50, and 100 μg NPs, respectively. (F−I) Primary human NY-ESO-1-specific T cells were added to DCs cultured in alginate cryogels, and the % of CD25-expressing CD8$^+$ T cells at 24 h (F), % of proliferated CD8$^+$ T cells at 72 h (G), and mean cycle of CD8$^+$ T cells at 72 h (H) were analyzed, together with their IFNγ production after 48 h (I). (B,E−I) $n = 3$ in three independent experiments. (C,D) $n = 2$ in two independent experiments. (B−I) Stars indicate significance compared to 0 μg, unless indicated otherwise. (B−E) Data were analyzed using a two-way ANOVA and Sidak's multiple comparison test. (F−K) Data were analyzed using a two-way ANOVA and Dunnett's multiple comparison tests (F−K) on log-transformed data (F,G).

of DCs following s.c. administration and subsequent T cell priming within the scaffolds and in the draining lymph nodes *in vivo* as was shown before.[3−8] Confocal imaging after 24 h revealed that BMDCs had taken up the A647 dye that was

https://doi.org/10.1021/acsbiomaterials.0c01648
ACS Biomater. Sci. Eng. 2021, 7, 5622−5632

encapsulated within NPs entrapped within the cryogel polymer walls (Figure 2A). Quantification by flowcytometry demonstrated that more than 90% of BMDCs were positive for the A647 dye after 24 h when 50 or 100 μg of NPs was incorporated (Figure S4A), which increased to almost 100% after 48 h of incubation (Figure 2B). The total amount of NPs taken up by BMDCs from scaffolds, as measured by the A647 geometric mean fluorescence intensity (MFI) was, however, significantly lower compared to when NPs are freely available (MFI of 1232 ± 216 for BMDCs cultured in cryogels loaded with 100 μg of NP *vs* a MFI of 12,741 ± 1181 for BMDCs exposed to freely available NPs) (Figures 2C and S4B), indicating that the cryogel walls present a barrier for NP uptake by DCs.

We next investigated whether OVA/TLR NP uptake results in BMDC activation. Although DCs did not get activated when cultured in NP-free cryogels, we observed increasing expression levels of activation markers CD40 (Figure 2D), CD80, and CD86 (Figure S5), and a significant increase in the percentage of $CD80^+CD86^+$ cells (Figure 2E) when BMDCs were cultured in NP-loaded alginate cryogels. At the same time, BMDCs cultured in NP-loaded cryogels expressed high levels of pro-inflammatory cytokines (TNFα and IL-6) (Figure 2F,G). This shows that even though DCs take up fewer NPs from alginate scaffolds compared to those with free NPs, strong DC maturation is induced which is comparable to that of DCs exposed to OVA/TLR NPs in suspension. We assume that the amount of NPs that is taking up by DCs in the NP-loaded cryogels is sufficient to overcome the threshold for DC activation. RGD-functionalization of the OVA/TLR-loaded alginate cryogels did not affect BMDC activation, suggesting that BMDCs have sufficient opportunities to interact with the scaffold network and obtain NPs without these integrin-binding sites *in vitro*. Addition of integrin-binding motifs such as RGD is however likely to have an important role in supporting immune cell adhesion and infiltration *in vivo*.[31] Taken together, these data underline the potential of alginate cryogels to establish a depot of cargo-loaded NPs which DCs are able to take up.

To determine whether BMDCs activated within NP-loaded scaffolds had been able to take up and cross-present antigen, we tested their ability to prime antigen-specific T cells. BMDCs were cultured in OVA/TLR NP-loaded alginate cryogels for 24 h, after which CFSE-labelled OT-I T cells, which express a transgenic T cell receptor specific for the OVA epitope SIINFEKL, were added on top. BMDCs stimulated by NP-loaded scaffolds induced vigorous proliferation in over 80% of OT-I T cells, similar to BMDCs stimulated with free NPs (Figure 3A,B). At least 50 μg of NPs were required per scaffold to induce robust T cell expansion. These T cells also produced IFNγ, although at lower levels than T cells activated by BDMCs stimulated with freely available NPs (Figure 3C). We did not observe significant differences in T cell responses induced in RGD-functionalized adhesive cryogels and non-functionalized cryogels, which correspond to the similar levels of BMDC activation in these scaffolds (Figure 2D−G).

These results clearly indicate that mouse BMDCs are able to take up NPs from dense alginate scaffold walls but to a lower extent compared to when NPs are freely available. Despite the decreased uptake of NPs, BMDCs cultured in alginate cryogels acquire a highly activated phenotype and can expand antigen-specific T cells efficiently.

Finally, we set out to study the importance of having the antigens/adjuvants encapsulated within NP in the scaffold walls. As such, we compared alginate cryogels containing OVA/TLR NP with alginate cryogels prepared with the addition of soluble OVA/TLR before the cryogel gelation process. We observed that the cargo was retained longer within the alginate cryogels when it was encapsulated within PLGA NPs as the release of TLR ligand R848 was delayed (Figure S6). Next, we took these cryogels and added FLT3L DCs directly or after incubating the cryogels in complete medium for 1 or 2 days. This way we could study the impact of cargo release from the cryogels when DCs do not enter the scaffold directly, which reflects the situation when such cryogels are administered *in vivo*.[4] The encapsulation of cargo within NP instead of being present within the alginate scaffold walls in the soluble form only had a minor impact on the upregulation of activation markers and IL-12 production by FLT3L DCs (Figure S7). We did however observe that OT-I T cell activation and expansion was higher when OVA/TLR were presented in NP-loaded alginate cryogels, especially when we waited 1 or 2 days before adding the DCs (Figure S8). This underlines the added benefit of using NP to incorporate antigens and adjuvants within alginate cryogels in order to tune and slow down the release of cargo.

Human DC and T Cell Activation in NY-ESO-1/TLR NP-Loaded Cryogels. We next evaluated activation of human DCs and subsequent priming of primary human antigen-specific T cells in NP-loaded alginate cryogels to evaluate the potential of clinical translation of this synthetic platform. Alginate cryogels loaded with NPs encapsulating NY-ESO-1 long peptide, TLR ligands polyI/C and R848, and A647 (Figure S1B,D) were produced, and fluorescence measurements confirmed dose-dependent incorporation of the NPs (Figure 4A). Primary monocyte-derived DCs (moDCs) from HLA-$A2.1^+$ donors cultured within NY-ESO-1/TLR NP-loaded cryogels were able to take up NPs as up to 100% of moDCs were positive for the A647 dye after 48 h of incubation (Figures 4B and S4C). Again, we observed reduced NP uptake in alginate cryogels compared to freely available NPs (Figures 4C and S4D). The uptake of NPs resulted in upregulation of activation marker CD40 on moDCs to a similar extent as moDCs stimulated with free NPs in a dose-dependent manner (Figure 4D,E), indicating that NY-ESO-1/TLR NP-loaded cryogels induce DC maturation.

To study antigen-specific T cell expansion in this setting, $CD8^+$ T cells from the same HLA-$A2.1^+$ donor were transfected with a NY-ESO-1-specific TCR with high efficiency (Figure S9A). When these antigen-specific T cells were cultured with moDCs in control cryogels containing empty NPs or when they were cultured in NP-loaded cryogels without DCs, we did not observe any upregulation of activation marker CD25 or T cell proliferation (Figure S9B−D). On the contrary, when NY-ESO-1-specific T cells were co-cultured with moDCs within NY-ESO-1 NP-loaded alginate cryogels, we observed a significant increase in CD25 expression (Figure 4F), strong induction of T cell proliferation (Figure 4G,H), and an upregulation of IFNγ production (Figure 4I). These data confirm our observations for OVA/TLR NPs, showing that alginate cryogels comprise a versatile platform that can be used to form a depot of antigen/adjuvant-loaded NPs to expand both human and mouse antigen-specific T cells in various *in vitro* models.

https://doi.org/10.1021/acsbiomaterials.0c01648
ACS Biomater. Sci. Eng. 2021, 7, 5622−5632

DISCUSSION

The ability of cancer vaccines to induce potent antitumor immune responses heavily relies on adequate delivery of tumor-associated antigens and adjuvants to DCs in the right context. NP-based delivery systems can be applied to control biomolecule release profiles, improve cargo half-life, and boost (co-)delivery of antigens and adjuvants to DCs, which is critical to achieve strong DC activation. Here, we developed a novel strategy to stimulate DCs within macroporous scaffolds by incorporating antigen/adjuvant-loaded PLGA NP into the polymer walls of the scaffold. This alternative approach to deliver stimulatory signals to DC within 3D scaffolds results in strong DC activation and acquisition of antigen-specific T cell-priming abilities.

Biomaterial-based scaffolds applied as platforms for cancer vaccination promote sustained availability of antigens and adjuvants and provide a supportive environment for immune cell priming. DCs can be recruited and activated *in vivo* through incorporation of GM-CSF and CpG oligodeoxynucleotides. These scaffold-based vaccines are able to induce robust anticancer immune responses that are superior to subcutaneous administration of soluble antigens and adjuvants without scaffolds.[3−8]

We expand on this platform by encapsulating biodegradable PLGA NP loaded with synthetic tumor-associated antigens and DC-activating TLR ligands into scaffold walls with high efficiency in a straightforward manner. NP-loaded alginate cryogels were prepared that preserve their favorable mechanical properties and can thus serve as a depot for the antigen/adjuvant-loaded NP. The main advantage of using pre-defined synthetic tumor antigens as a source of antigen rather than tumor lysate[3,32] or irradiated tumor cells[4] is that it is a fully synthetic approach. This precludes the time and regulatory burden associated with culturing of whole tumor cells, avoids the limited immunogenicity associated with tumor lysates, prevents the suppressive effects that tumor lysates can have on DCs,[33,34] and eliminates the potential risk of inducing autoimmunity against self-antigens.[35−37]

This alternative approach of providing DCs with activating signals through NPs incorporated into the polymer walls has other advantages as well. Incorporating antigens and adjuvants into NPs that are loaded into the scaffold walls, rather than adsorbing the proteins directly onto the scaffold surface[5,8] or attaching them in a covalent manner[6] offers the opportunity for another level of spatiotemporal control over the presentation of activating cues to DCs. Based on the type and formulation of the NP that is used, the release profile of the components can be tuned.[10] For instance, NP can be prepared that degrade in response to a change in pH, due to the presence of enzymes or by oxidation in order to more precisely control the spatiotemporal release kinetics of the encapsulated cargo. A particle-based approach furthermore benefits from the inherent uptake of particulate matter by DCs, thereby potentially improving uptake of cargo,[11,12] favoring co-delivery of components,[13−17] and enhancing cross-presentation[12,18−20] of antigens and adjuvants presented within biomaterial-based scaffolds. To fully apprehend the behavior of PLGA NP-loaded alginate cryogels, the exact kinetics of DC influx and NP uptake, NP degradation, diffusion of cargo out of NP, and the passive release of NPs for different types of particles from the scaffold walls will need to be established. This characterization will be pivotal to gain more insights into the (tuneable) spatiotemporal characteristics of the NP-loaded scaffold-based cancer vaccine platform, which can have a large impact on the resulting immune response. Covalent attachment or slow release of antigens and adjuvants can, for instance, improve bioavailability for long-term DC stimulation and promote memory formation,[7,8] although care must be taken as persisting depots of antigens for DCs have been reported to induce dysfunctional T cells or locally sequester effector T cells.[38,39] Side-by-side comparison of various strategies to deliver antigens and adjuvants to DCs within 3D biomaterial-based scaffolds will in the future be required to delineate per application what approach is most relevant.

CONCLUSIONS

We have successfully developed an alternative strategy to stimulate DCs within macroporous cryogels by incorporating antigen/adjuvant-loaded NPs into the polymer walls of the scaffold. Through careful optimization, NP-loaded alginate cryogels were prepared that preserve their favorable mechanical properties and can thus serve as an injectable depot for the antigen/adjuvant-loaded NPs. This work provides an important addition to the toolbox of scaffold-based cancer vaccination approaches by combining the advantage of particle-based cargo delivery to DCs with the favorable properties of 3D biomaterial-based scaffolds. In the future, various particle-based formulations could be introduced into the injectable cryogels in order to gain more control over the spatiotemporal release kinetics of antigens and adjuvants.

ASSOCIATED CONTENT

Supporting Information

The Supporting Information is available free of charge at https://pubs.acs.org/doi/10.1021/acsbiomaterials.0c01648.

Characterization of MA-alginate and PLGA NPs; mechanical properties of alginate cryogels affected by incorporation of NPs; macroporous alginate cryogels supporting DC survival and migration; uptake of PLGA NPs by DCs after 24 h; mouse BMDCs cultured in OVA/TLR NP-loaded alginate cryogels; release of TLR ligand R848 measured by HPLC and expression as the % of the total amount of R848; comparison of mouse FLT3L DCs cultured in OVA/TLR NP-loaded alginate cryogels versus alginate cryogels containing soluble OVA/TLR added during cryogelation; activation of antigen-specific OT-I T cells in response to mouse FLT3L DCs; and high transfection efficiency and low background activation of NY-ESO-1 TCR-transfected primary T cells (PDF)

AUTHOR INFORMATION

Corresponding Author

Martijn Verdoes − *Department of Tumor Immunology, Radboud Institute for Molecular Life Sciences, Radboud University Medical Center, Nijmegen 6525 GA, Netherlands; Institute for Chemical Immunology, Nijmegen 6525 GA, Netherlands;* orcid.org/0000-0001-8753-3528; Email: martijn.verdoes@radboudumc.nl

Authors

Jorieke Weiden − *Department of Tumor Immunology, Radboud Institute for Molecular Life Sciences and Division of Immunotherapy, Oncode Institute, Radboud University*

https://doi.org/10.1021/acsbiomaterials.0c01648
ACS Biomater. Sci. Eng. 2021, 7, 5622−5632

Medical Center, Nijmegen 6525 GA, Netherlands; Institute for Chemical Immunology, Nijmegen 6525 GA, Netherlands; orcid.org/0000-0002-2485-0590

Marjolein Schluck − *Department of Tumor Immunology, Radboud Institute for Molecular Life Sciences and Division of Immunotherapy, Oncode Institute, Radboud University Medical Center, Nijmegen 6525 GA, Netherlands; Institute for Chemical Immunology, Nijmegen 6525 GA, Netherlands*

Melina Ioannidis − *Department of Tumor Immunology, Radboud Institute for Molecular Life Sciences, Radboud University Medical Center, Nijmegen 6525 GA, Netherlands*

Eric A. W. van Dinther − *Department of Tumor Immunology, Radboud Institute for Molecular Life Sciences and Division of Immunotherapy, Oncode Institute, Radboud University Medical Center, Nijmegen 6525 GA, Netherlands*

Mahboobeh Rezaeeyazdi − *Department of Chemical Engineering, Northeastern University, Boston, Massachusetts 02115, United States*

Fawad Omar − *Department of Tumor Immunology, Radboud Institute for Molecular Life Sciences, Radboud University Medical Center, Nijmegen 6525 GA, Netherlands*

Juulke Steuten − *Department of Tumor Immunology, Radboud Institute for Molecular Life Sciences, Radboud University Medical Center, Nijmegen 6525 GA, Netherlands*

Dion Voerman − *Department of Tumor Immunology, Radboud Institute for Molecular Life Sciences and Division of Immunotherapy, Oncode Institute, Radboud University Medical Center, Nijmegen 6525 GA, Netherlands; Institute for Chemical Immunology, Nijmegen 6525 GA, Netherlands*

Jurjen Tel − *Department of Biomedical Engineering, Laboratory of Immunoengineering and Institute for Complex Molecular Systems, Eindhoven University of Technology, Eindhoven 5600 MB, Netherlands*

Mustafa Diken − *TRON-Translational Oncology at the University Medical Center of the Johannes Gutenberg University gGmbH, Mainz 55131, Germany*

Sidi A. Bencherif − *Department of Chemical Engineering, Northeastern University, Boston, Massachusetts 02115, United States; Department of Bioengineering, Northeastern University, Boston, Massachusetts 02115, United States; Harvard John A. Paulson School of Engineering and Applied Sciences, Harvard University, Cambridge, Massachusetts 02138, United States; Biomechanics and Bioengineering (BMBI), UTC CNRS UMR 7338, University of Technology of Compiègne, Sorbonne University, Compiègne 60203, France;* orcid.org/0000-0002-7704-5608

Carl G. Figdor − *Department of Tumor Immunology, Radboud Institute for Molecular Life Sciences and Division of Immunotherapy, Oncode Institute, Radboud University Medical Center, Nijmegen 6525 GA, Netherlands; Institute for Chemical Immunology, Nijmegen 6525 GA, Netherlands*

Complete contact information is available at: https://pubs.acs.org/10.1021/acsbiomaterials.0c01648

Author Contributions

J.W., M.S., C.G.F., and M.V. conceived and planned the experiments. J.W., M.S., M.I., E.A.W.v.D., M.R., F.O., J.S., and D.V. performed the experiments. J.T., S.A.B., C.G.F., and M.V. were involved in supervision and interpretation of the data. M.D. provided the TCR constructs. J.W. drafted the manuscript and designed the figures with consultation of M.S., J.T., S.A.B., C.G.F. and M.V. All authors have given approval to the final version of the manuscript.

Notes

The authors declare no competing financial interest.

■ ACKNOWLEDGMENTS

The authors thank Yusuf Dölen for setting up the CD8+ T cell transfection system. This work was supported by a PhD grant from the NWO Gravity Program Institute for Chemical Immunology and the Oncode Institute. C.F. is recipient of the NWO Spinoza award and ERC Adv. Grants ARTimmune (834618) and Pathfinder (269019). M.V. is recipient of ERC Starting grant CHEMCHECK (679921) and a Gravity Program Institute for Chemical Immunology tenure track grant by NWO.

■ REFERENCES

(1) Gardner, A.; Ruffell, B. Dendritic Cells and Cancer Immunity. *Trends Immunol.* **2016**, *37*, 855−865.

(2) Weiden, J.; Tel, J.; Figdor, C. G. Synthetic Immune Niches for Cancer Immunotherapy. *Nat. Rev. Immunol.* **2018**, *18*, 212.

(3) Ali, O. A.; Huebsch, N.; Cao, L.; Dranoff, G.; Mooney, D. J. Infection-Mimicking Materials to Program Dendritic Cells in Situ. *Nat. Mater.* **2009**, *8*, 151−158.

(4) Bencherif, S. A.; Warren Sands, R.; Ali, O. A.; Li, W. A.; Lewin, S. A.; Braschler, T. M.; Shih, T.-Y.; Verbeke, C. S.; Bhatta, D.; Dranoff, G.; Mooney, D. J. Injectable Cryogel-Based Whole-Cell Cancer Vaccines. *Nat. Commun.* **2015**, *6*, 7556.

(5) Kim, J.; Li, W. A.; Choi, Y.; Lewin, S. A.; Verbeke, C. S.; Dranoff, G.; Mooney, D. J. Injectable, Spontaneously Assembling, Inorganic Scaffolds Modulate Immune Cells in Vivo and Increase Vaccine Efficacy. *Nat. Biotechnol.* **2015**, *33*, 64−72.

(6) Li, A. W.; Sobral, M. C.; Badrinath, S.; Choi, Y.; Graveline, A.; Stafford, A. G.; Weaver, J. C.; Dellacherie, M. O.; Shih, T.-Y.; Ali, O. A.; Kim, J.; Wucherpfennig, K. W.; Mooney, D. J. A Facile Approach to Enhance Antigen Response for Personalized Cancer Vaccination. *Nat. Mater.* **2018**, *17*, 528−534.

(7) Dellacherie, M. O.; Li, A. W.; Lu, B. Y.; Mooney, D. J. Covalent Conjugation of Peptide Antigen to Mesoporous Silica Rods to Enhance Cellular Responses. *Bioconjugate Chem.* **2018**, *29*, 733−741.

(8) Sinha, A.; Choi, Y.; Nguyen, M. H.; Nguyen, T. L.; Choi, S. W.; Kim, J. A 3D Macroporous Alginate Graphene Scaffold with an Extremely Slow Release of a Loaded Cargo for In Situ Long-Term Activation of Dendritic Cells. *Adv. Healthcare Mater.* **2019**, *8*, 1800571.

(9) Roth, G. A.; Gale, E. C.; Alcántara-Hernández, M.; Luo, W.; Axpe, E.; Verma, R.; Yin, Q.; Yu, A. C.; Lopez Hernandez, H.; Maikawa, C. L.; Smith, A. A. A.; Davis, M. M.; Pulendran, B.; Idoyaga, J.; Appel, E. A. Injectable Hydrogels for Sustained Codelivery of Subunit Vaccines Enhance Humoral Immunity. *ACS Cent. Sci.* **2020**, *6*, 1800−1812.

(10) Cruz, L. J.; Tacken, P. J.; Eich, C.; Rueda, F.; Torensma, R.; Figdor, C. G. Controlled Release of Antigen and Toll-like Receptor Ligands from PLGA Nanoparticles Enhances Immunogenicity. *Nanomedicine* **2017**, *12*, 491−510.

(11) Macri, C.; Dumont, C.; Johnston, A. P.; Mintern, J. D. Targeting Dendritic Cells: A Promising Strategy to Improve Vaccine Effectiveness. *Clin. Transl. Immunol.* **2016**, *5*, No. e66.

(12) Hanlon, D.; Hanlon, D. J.; Sharp, F. A.; Hong, E.; Khalil, D.; Robinson, E.; Tigelaar, R.; Fahmy, T. M.; Edelson, R. L. Targeting Human Dendritic Cells via DEC-205 Using PLGA Nanoparticles Leads to Enhanced Cross-Presentation of a Melanoma-Associated Antigen. *Int. J. Nanomed.* **2014**, *9*, 5231−5246.

(13) Dölen, Y.; Kreutz, M.; Gileadi, U.; Tel, J.; Vasaturo, A.; van Dinther, E. A. W.; van Hout-Kuijer, M. A.; Cerundolo, V.; Figdor, C. G. Co-Delivery of PLGA Encapsulated Invariant NKT Cell Agonist

with Antigenic Protein Induce Strong T Cell-Mediated Antitumor Immune Responses. *Oncoimmunology* **2015**, *5*, No. e1068493.
(14) Wilson, J. T.; Keller, S.; Manganiello, M. J.; Cheng, C.; Lee, C.-C.; Opara, C.; Convertine, A.; Stayton, P. S. PH-Responsive Nanoparticle Vaccines for Dual-Delivery of Antigens and Immunostimulatory Oligonucleotides. *ACS Nano* **2013**, *7*, 3912−3925.
(15) Fischer, N. O.; Rasley, A.; Corzett, M.; Hwang, M. H.; Hoeprich, P. D.; Blanchette, C. D. Colocalized Delivery of Adjuvant and Antigen Using Nanolipoprotein Particles Enhances the Immune Response to Recombinant Antigens. *J. Am. Chem. Soc.* **2013**, *135*, 2044−2047.
(16) Diwan, M.; Tafaghodi, M.; Samuel, J. Enhancement of Immune Responses by Co-Delivery of a CpG Oligodeoxynucleotide and Tetanus Toxoid in Biodegradable Nanospheres. *J. Controlled Release* **2002**, *85*, 247−262.
(17) Tacken, P. J.; Zeelenberg, I. S.; Cruz, L. J.; van Hout-Kuijer, M. A.; van de Glind, G.; Fokkink, R. G.; Lambeck, A. J. A.; Figdor, C. G. Targeted Delivery of TLR Ligands to Human and Mouse Dendritic Cells Strongly Enhances Adjuvanticity. *Blood* **2011**, *118*, 6836−6844.
(18) Audran, R.; Peter, K.; Dannull, J.; Men, Y.; Scandella, E.; Groettrup, M.; Gander, B.; Corradin, G. Encapsulation of Peptides in Biodegradable Microspheres Prolongs Their MHC Class-I Presentation by Dendritic Cells and Macrophages in Vitro. *Vaccine* **2003**, *21*, 1250−1255.
(19) Shen, H.; Ackerman, A. L.; Cody, V.; Giodini, A.; Hinson, E. R.; Cresswell, P.; Edelson, R. L.; Saltzman, W. M.; Hanlon, D. J. Enhanced and Prolonged Cross-Presentation Following Endosomal Escape of Exogenous Antigens Encapsulated in Biodegradable Nanoparticles. *Immunology* **2006**, *117*, 78−88.
(20) Lim, Y. T.; Song, C.; Noh, Y.-W. Polymer Nanoparticles for Cross-Presentation of Exogenous Antigens and Enhanced Cytotoxic T-Lymphocyte Immune Response. *Int. J. Nanomed.* **2016**, *11*, 3753−3764.
(21) Clawson, C.; Huang, C.-T.; Futalan, D.; Martin Seible, D.; Saenz, R.; Larsson, M.; Ma, W.; Minev, B.; Zhang, F.; Ozkan, M.; Ozkan, C.; Esener, S.; Messmer, D. Delivery of a Peptide via Poly(D,L-Lactic-Co-Glycolic) Acid Nanoparticles Enhances Its Dendritic Cell-Stimulatory Capacity. *Nanomedicine* **2010**, *6*, 651−661.
(22) de Jong, S.; Chikh, G.; Sekirov, L.; Raney, S.; Semple, S.; Klimuk, S.; Yuan, N.; Hope, M.; Cullis, P.; Tam, Y. Encapsulation in Liposomal Nanoparticles Enhances the Immunostimulatory, Adjuvant and Anti-Tumor Activity of Subcutaneously Administered CpG ODN. *Cancer Immunol. Immunother.* **2007**, *56*, 1251−1264.
(23) Bencherif, S. A.; Sands, R. W.; Bhatta, D.; Arany, P.; Verbeke, C. S.; Edwards, D. A.; Mooney, D. J. Injectable Preformed Scaffolds with Shape-Memory Properties. *Proc. Natl. Acad. Sci. U.S.A.* **2012**, *109*, 19590−19595.
(24) Eggermont, L. J.; Rogers, Z. J.; Colombani, T.; Memic, A.; Bencherif, S. A. Injectable Cryogels for Biomedical Applications. *Trends Biotechnol.* **2020**, *38*, 418−431.
(25) Colombani, T.; Eggermont, L. J.; Hatfield, S. M.; Rezaeeyazdi, M.; Memic, A.; Sitkovsky, M. V.; Bencherif, S. A. Oxygen-Generating Cryogels Restore T Cell-Mediated Cytotoxicity in Hypoxic Tumor-sTitle. **2020**, bioRxiv 2020.10.08.329805.
(26) Weiden, J.; Voerman, D.; Dölen, Y.; Das, R. K.; van Duffelen, A.; Hammink, R.; Eggermont, L. J.; Rowan, A. E.; Tel, J.; Figdor, C. G. Injectable Biomimetic Hydrogels as Tools for Efficient T Cell Expansion and Delivery. *Front. Immunol.* **2018**, *9*, 2798.
(27) Qiu, L.; Valente, M.; Dolen, Y.; Jäger, E.; Beest, M. T.; Zheng, L.; Figdor, C. G.; Verdoes, M. Endolysosomal-Escape Nanovaccines through Adjuvant-Induced Tumor Antigen Assembly for Enhanced Effector CD8+ T Cell Activation. *Small* **2018**, *14*, 1703539.
(28) Sarker, B.; Boccaccini, A. R. *Alginate Utilization in Tissue Engineering and Cell Therapy*; Springer, 2018; pp 121−155.
(29) Ruoslahti, E. RGD and Other Recognition Sequences for Integrins. *Annu. Rev. Cell Dev. Biol.* **1996**, *12*, 697−715.
(30) Bauleth-Ramos, T.; Shih, T.; Shahbazi, M.; Najibi, A. J.; Mao, A. S.; Liu, D.; Granja, P.; Santos, H. A.; Sarmento, B.; Mooney, D. J. Acetalated Dextran Nanoparticles Loaded into an Injectable Alginate Cryogel for Combined Chemotherapy and Cancer Vaccination. *Adv. Funct. Mater.* **2019**, *29*, 1903686.
(31) Hersel, U.; Dahmen, C.; Kessler, H. RGD Modified Polymers: Biomaterials for Stimulated Cell Adhesion and Beyond. *Biomaterials* **2003**, *24*, 4385−4415.
(32) Phuengkham, H.; Song, C.; Um, S. H.; Lim, Y. T. Implantable Synthetic Immune Niche for Spatiotemporal Modulation of Tumor-Derived Immunosuppression and Systemic Antitumor Immunity: Postoperative Immunotherapy. *Adv. Mater.* **2018**, *30*, 1706719.
(33) Hatfield, P.; Merrick, A. E.; West, E.; O'Donnell, D.; Selby, P.; Vile, R.; Melcher, A. A. Optimization of Dendritic Cell Loading with Tumor Cell Lysates for Cancer Immunotherapy. *J. Immunother.* **2008**, *31*, 620−632.
(34) González, F. E.; Gleisner, A.; Falcón-Beas, F.; Osorio, F.; López, M. N.; Salazar-Onfray, F. Tumor Cell Lysates as Immunogenic Sources for Cancer Vaccine Design. *Hum. Vaccines Immunother.* **2014**, *10*, 3261−3269.
(35) Ludewig, B.; Ochsenbein, A. F.; Odermatt, B.; Paulin, D.; Hengartner, H.; Zinkernagel, R. M. Immunotherapy with Dendritic Cells Directed against Tumor Antigens Shared with Normal Host Cells Results in Severe Autoimmune Disease. *J. Exp. Med.* **2000**, *191*, 795−804.
(36) Uchi, H.; Stan, R.; Turk, M. J.; Engelhorn, M. E.; Rizzuto, G. A.; Goldberg, S. M.; Wolchok, J. D.; Houghton, A. N. Unraveling the Complex Relationship between Cancer Immunity and Autoimmunity: Lessons from Melanoma and Vitiligo. *Adv. Immunol.* **2006**, *90*, 215−241.
(37) Jacobs, J. F. M.; Aarntzen, E. H. J. G.; Sibelt, L. A. G.; Blokx, W. A.; Boullart, A. C. I.; Gerritsen, M.-J.; Hoogerbrugge, P. M.; Figdor, C. G.; Adema, G. J.; Punt, C. J. A.; de Vries, I. J. M. Vaccine-Specific Local T Cell Reactivity in Immunotherapy-Associated Vitiligo in Melanoma Patients. *Cancer Immunol. Immunother.* **2009**, *58*, 145−151.
(38) Hailemichael, Y.; Dai, Z.; Jaffarzad, N.; Ye, Y.; Medina, M. A.; Huang, X.-F.; Dorta-Estremera, S. M.; Greeley, N. R.; Nitti, G.; Peng, W.; Liu, C.; Lou, Y.; Wang, Z.; Ma, W.; Rabinovich, B.; Sowell, R. T.; Schluns, K. S.; Davis, R. E.; Hwu, P.; Overwijk, W. W. Persistent Antigen at Vaccination Sites Induces Tumor-Specific $CD8^+$ T Cell Sequestration, Dysfunction and Deletion. *Nat. Med.* **2013**, *19*, 465−472.
(39) Hailemichael, Y.; Woods, A.; Fu, T.; He, Q.; Nielsen, M. C.; Hasan, F.; Roszik, J.; Xiao, Z.; Vianden, C.; Khong, H.; Singh, M.; Sharma, M.; Faak, F.; Moore, D.; Dai, Z.; Anthony, S. M.; Schluns, K. S.; Sharma, P.; Engelhard, V. H.; Overwijk, W. W. Cancer Vaccine Formulation Dictates Synergy with CTLA-4 and PD-L1 Checkpoint Blockade Therapy. *J. Clin. Invest.* **2018**, *128*, 1338−1354.

https://doi.org/10.1021/acsbiomaterials.0c01648
ACS Biomater. Sci. Eng. 2021, 7, 5622−5632